



Improved dose compensation model owing to short irradiation interruption time for hypoxic tumor using a microdosimetric kinetic model

Daisuke Kawahara

Department of Radiation Oncology, Institute of Biomedical and Health Sciences, Hiroshima University, Hiroshima, Japan

ABSTRACT

Background: The objective was to enhance the biological compensation factor related to irradiation interruption in a short time (short irradiation interruption) in hypoxic tumors using a refined microdosimetric kinetic model (MKM) for photon radiation therapy.

Materials and methods: The biological dose differences were calculated for CHO-K1 cells exposed to a photon beam, considering interruptions of (τ) of 0-120 min and pO_2 at oxygen levels of 0.075-160 mm Hg. The interrupted dose fraction (IDF) was defined as the percentage ratio of the dose delivered before short irradiation interruption to the total dose, which ranged from 10-90%. The compensated dose was calculated based on an IDF of 10-90% for a dose of 2-8 Gy and oxygen levels of 0.075-160 mm Hg.

Results: The Δ with and without short irradiation interruption was more pronounced with a higher dose and increased pO_2 . It exceeded 3% between IDF of 50% and either 10% or 90% and occurred more than $\tau = 50$ min at 0.075 mm Hg, $\tau = 20$ min at 3 mm Hg, $\tau = 20$ min at 8 mm Hg, $\tau = 20$ min at 15 mm Hg, $\tau = 20$ min at 38 mm Hg, and $\tau = 20$ min at 160 mm Hg. The dose compensation factor was greater at higher IDF rates.

Conclusion: The biological dose decreased with longer interruption times and higher oxygen concentrations. The improved model can compensate for the biological doses at various oxygen concentrations.

Advances in knowledge: The current study improved the dose compensation method for the decrease in the biological effect owing to short irradiation interruption by considering the oxygen concentration.

Key words: radiotherapy; microdosimetric kinetic model; hypoxia; interruption time; dose compensation model

Rep Pract Oncol Radiother 2024;29(3):271-279

Introduction

Treatment techniques and dose delivery have improved in radiotherapy. Intensity-modulated radiotherapy (IMRT) technique employs variable intensities across multiple beams, leading to highly conformal dose distributions. IMRT often re-

quires multiple beams that increases treatment delivery time [1, 2]. Recently, the volumetric modulated arc therapy (VMAT) technique has allowed treatment using one or two arcs [3]. This technique reduces the dose delivery time in comparison with the IMRT technique. Stereotactic radiosurgery (SRS) and stereotactic body radiotherapy (SBRT)

Address for correspondence: Daisuke Kawahara, Ph.D., Daisuke Kawahara, Department of Radiation Oncology, Institute of Biomedical and Health Sciences, 1-2-3 Kasumi, Minami-ku, Hiroshima-shi, Hiroshima, Japan, tel: +81-82-257-1545, fax: +81-82-257-1546; e-mail: daika99@hiroshima-u.ac.jp

This article is available in open access under Creative Common Attribution-Non-Commercial-No Derivatives 4.0 International (CC BY-NC-ND 4.0) license, allowing to download articles and share them with others as long as they credit the authors and the publisher, but without permission to change them in any way or use them commercially

involve a large dose per fraction that requires a longer dose delivery time than conventional radiotherapy. Recently, SBRT has been combined with a flattening filter-free (FFF) beam that uses a non-uniform beam and can reduce the treatment delivery time [4, 5].

Prolonged delivery time affects radiobiological damage. Elkind et al. introduced sublethal damage repair (SLDR) in which cell death tends to decrease with a longer dose delivery time [5]. Nakano et al. reported a difference in dose delivery times between FFF and flattened filter (FF) beams [6]. They simulated radiobiological effectiveness using a microdosimetric kinetic model (MKM). In clinical treatments, short irradiation interruptions can occur by increasing the interval between treatment beams through couch rotations with noncoplanar beams, increasing the interval between multiple beams, and unscheduled down-time (DT) with machine failures. These interruptions can extend delivery time. We proposed a dose compensation method for irradiation interruptions in a short time using the MKM [7]. However, in clinical radiotherapy, the radiosensitivity of tumor cells decreased in the hypoxic region; this plays an important role in malignant progression. Hall et al. reported that oxygen concentrations below 20% induced radio-resistance [8]. Tinganelli et al. showed that the cell survival curve changes depending on the period during which the cells are exposed to hypoxic conditions [9]. Thus, the survival curve parameters should be fitted under various oxygen conditions. However, this approach is inefficient. Therefore, the development of a model that can determine the model parameters from the limited experimental model parameters is required.

The current study improved the MKM by considering oxygen dose enhancement in hypoxic tumors. Moreover, it was used to evaluate the biological dose by varying the dose-delivery time in hypoxic tumors.

Materials and methods

Survival fraction in the MKM

The survival fraction of cells was modeled by Hakins et al. and Inaniwa et al. with the MKM that used the dose by a domain of divided cell nucleus [10, 11]. It is defined as follows:

$$-\ln S = \left(\alpha_0 + \frac{y_D}{\rho \pi r_d^2} \beta_0 \right) D + \beta' D^2 \quad (1)$$

where y_D denotes the dose mean energy (keV/ μm), and α_0 is the proportionality factor to D [Gy^{-1}] and β_0 is the proportionality factor to D^2 [Gy^{-2}] that are obtained by the survival fraction in the LQ model. These parameters were used for the CHO-K1 cells, which was listed in Table 1 [12]. Radius r_d and density ρ of the domain values were 0.23 μm and 1.0 g/cm^3 , respectively. Matsuya et al. modified the MKM with the oxygen effect as follows:

$$-\ln S = \left(\alpha_0 + \frac{y_D}{\rho \pi r_d^2} \beta_0 \right) D' + \beta' D'^2 \quad (2)$$

where D' denotes the dose corrected by the oxygen effect ratio. It is estimated using the hypoxia reduction factor (HRF) that is the ratio of the doses for a specific iso-effect under a given oxygenation condition compared with the condition at 21% O_2 . The HRF is derived as follows:

$$\text{HRF} = \frac{mK + \text{O}_2[c]}{K + \text{O}_2[c]} \quad (3)$$

where m is the maximum HRF, and K is the oxygen partial pressure at which the HRF is half the maximum value. The values of m and K were 2.7 and 0.002, respectively, and were fitted to the experimental data obtained by Paul-Gilloteaux et al. [13] $\text{O}_2[c]$ is the oxygen level at 0.075 mm Hg (hypoxia that causes tumor death), 3 mm Hg (radiobiological hypoxia), 8 mm Hg (pathological hypoxia), 15 mm Hg (physiological hypoxia), 38 mm Hg (physoxia), and 160 mm Hg (normal atmospheric pressure) [14]. The D' can be expressed as follows:

$$D' = \frac{D}{\text{HRF}} \quad (4)$$

Table 1. Calculation parameters. α_0 and β_0 are the proportionality factor to D [Gy^{-1}] and the proportionality factor to D^2 [Gy^{-2}]. y_D is the dose-mean lineal energy, and $T_{1/2}$ is the DNA repair half-time

Parameters	Mean	SD
α_0 (Gy^{-1})	0.175	0.023
β_0 (Gy^{-2})	0.033	-
$T_{1/2}$ [min]	22	-
y_D [keV/ μm]	2.32	0.04

From Eqs. (2) and (4), the survival fraction with the oxygen effect is as follows:

$$-\ln S = \left(\alpha_0 + \frac{y_D}{\rho \pi r_d^2} \beta_0 \right) \frac{D}{HRF} + \beta' \frac{D^2}{HRF} \quad (5)$$

where, the β' is defined as follows [11, 12]:

$$\beta' = \frac{2\beta}{(a+c)^2 T^2} \left[(a+c)T \frac{(1+e^{-2(a+c)t_r})}{(1-e^{-2(a+c)t_r})} - 1 + \frac{e^{-(a+c)T}(1-e^{-2(a+c)(t_r-T)})}{(1-e^{-2(a+c)t_r})} \right] \quad (6)$$

where T denotes the delivery time during irradiation, and (a + c) represents the potentially lethal lesion repair rate obtained by Matsuya et al [12]. Brenner et al. assumed that the potentially lethal lesion repair rate was equivalent to the primary rate λ which was obtained by the DNA repair half-time $T_{1/2}$ [15].

Physical dose and lineal energy distribution in PHITS

The physical dose and linear energy with a TrueBeam linear accelerator (Varian Medical Systems, Palo Alto, CA, USA) were obtained from the Monte Carlo calculation code particle and heavy ion transport code system (PHITS). Varian provided the phase space files above the jaw with a 6 MV X-ray beam; thus, the bottom of the secondary jaw was modeled [12]. The dose calculation was performed with a grid size of 2 mm and a photon history of 4.0×10^9 in the virtual water phantom ($20 \times 20 \times 20 \text{ cm}^3$). The photon and electron cut-off energies were set to 0.01 MeV and 0.7 MeV, respectively. The comparison of physical doses between the measurements and calculations was within 1.0% [16].

Biological dose with and without short irradiation interruptions

Biological doses (D_{bio}) with and without short irradiation interruptions are computed as follows [7, 11]:

$$D_{bio}^{w/o} = \left[\frac{\alpha_0}{2\beta_0} + \sqrt{\left(\frac{\alpha_0}{2\beta_0} \right)^2 + \frac{\left(\alpha_0 + \frac{y_D}{\rho \pi r_d^2} \beta' \right) D + \beta' D^2}{\beta_0}} \right] \quad (7)$$

$$D_{bio}^{with} = \left[\frac{\alpha_0}{2\beta_0} + \sqrt{\left(\frac{\alpha_0}{2\beta_0} \right)^2 + \frac{\left(\alpha_0 + \frac{y_D}{\rho \pi r_d^2} \beta' \right) D_1 + \left(\alpha_0 + \frac{y_D}{\rho \pi r_d^2} \beta' \right) D_2 + \beta_1 D_1^2 + \beta_2 D_2^2 + \beta_3 D_1 D_2}{\beta_0}} \right] \quad (8)$$

The number of short irradiation interruptions was one. D_1 denotes the physical dose at the first irradiation, and D_2 denotes the physical dose at the second irradiation. The total dose per fraction (D) was 2–8 Gy, as described in our previous study [7].

$$D = D_1 + D_2 \quad (9)$$

In this study, D was subdivided into D_1 and D_2 . Here, D_1 represented the dose delivered before short irradiation interruption and D_2 signified the dose post-interruption. To quantify the proportion of the dose at the point of short irradiation interruption, we introduced the interrupted dose fraction (IDF). The IDF is calculated as follows:

$$IDF = \frac{D_1}{D} \times 100 \quad (10)$$

This fraction provided percentages, such as 10%, 30%, 50%, 70%, and 90%, indicating the relative amount of the dose delivered before short irradiation interruption.

Coefficients β_1 , β_2 , and β_3 are defined as follows:

$$\beta_1 = \frac{2\beta}{(a+c)^2 T_1^2} \left[(a+c)T_1 \frac{(1+e^{-2(a+c)t_r})}{(1-e^{-2(a+c)t_r})} - 1 + \frac{e^{-(a+c)T_1}(1-e^{-2(a+c)(t_r-T_1)})}{(1-e^{-2(a+c)t_r})} \right] \quad (11)$$

$$\beta_2 = \frac{2\beta}{(a+c)^2 T_2^2} \left[(a+c)T_2 \frac{(1+e^{-2(a+c)t_r})}{(1-e^{-2(a+c)t_r})} - 1 + \frac{e^{-(a+c)T_2}(1-e^{-2(a+c)(t_r-T_2)})}{(1-e^{-2(a+c)t_r})} \right] \quad (12)$$

$$\beta_3 = \frac{2\beta}{(a+c)^2 T_1 T_2 (1-e^{-2(a+c)t_r})} \left\{ e^{-(a+c)(\tau+T_2)} + e^{-(a+c)\tau} - e^{-(a+c)(T_1+\tau+T_2)} + e^{-(a+c)(2t_r-\tau-T_2)} - e^{-(a+c)(2t_r-T_1-\tau-T_2)} \right\} \quad (13)$$

where t_r is the maximum time required for lethality and unreparability. In a previous study, the t_r for HSG tumors was 2.28 h [10]. Thus, the irradiation interruption time (τ) was varied to 0.1, 0.2, 0.3, 0.4, 0.5, 1, 2, 3, 4, 5, 10, 20, 30, 40, 50, 75, and 120 min. T_1 and T_2 denote the delivery times at the first and second irradiations, respectively. They are calculated using dose rate DR as follows:

$$T_1 = \frac{D_1}{DR} \quad (14)$$

$$T_2 = \frac{D_2}{DR} \quad (15)$$

In this study, a DR of 1.0 Gy/min was used. Using Eqs. 5, 7, and 8, D_{bio} with and without short irradiation interruptions can be expressed as follows:

$$D_{bio}^{w/o} = \left[-\frac{\alpha_0}{2\beta_0} + \sqrt{\left(\frac{\alpha_0}{2\beta_0}\right)^2 + \frac{\left(\alpha_0 + \frac{\gamma_D - \beta'}{\rho\pi r_d}\beta'\right) \frac{D}{HRF} + \beta' \frac{D^2}{HRF^2}}{\beta_0} \right] \quad (16)$$

$$D_{bio}^{with} = \left[-\frac{\alpha_0}{2\beta_0} + \sqrt{\left(\frac{\alpha_0}{2\beta_0}\right)^2 + \frac{\left(\alpha_0 + \frac{\gamma_D - \beta'}{\rho\pi r_d}\beta'\right) \frac{D_1}{HRF} + \left(\alpha_0 + \frac{\gamma_D - \beta'}{\rho\pi r_d}\beta'\right) \frac{D_2}{HRF} + \beta_1 D_1^2 + \beta_2 D_2^2 + \beta_3 D_1 D_2}}{\beta_0} \right] \quad (17)$$

The biological dose difference (Δ) is defined as follows:

$$\Delta = \frac{D_{bio}^{w/o} - D_{bio}^{with}}{D_{bio}^{with}} \quad (18)$$

Dose compensating factor for the biological dose with short irradiation interruption

The biological dose with short irradiation interruption is corrected as follows [17]:

$$D_{bio}^{w/o} = D_{1,bio}^{with} + D_{2,bio}^{with} + cD_{1,bio}^{with} \quad (19)$$

$cD_{1,bio}^{with}$ can be converted to a physical dose ($D_{1,phy}^{w/o}$) using Eq. (16) and is given by

$$D_{1,phy}^{w/o} = \frac{-\left(\frac{\alpha_0}{\beta'} + \frac{\beta_0}{\beta'} \frac{\gamma_D}{\rho\pi r_d}\right) + \sqrt{\left(\frac{\alpha_0}{\beta'} + \frac{\beta_0}{\beta'} \frac{\gamma_D}{\rho\pi r_d}\right)^2 + 4 \frac{\beta_0}{\beta'} c \frac{D_{1,bio}^{with}}{HRF} \left(c \frac{D_{1,bio}^{with}}{HRF} + \frac{\alpha_0}{\beta_0}\right)}}{2} \quad (20)$$

The dose compensating factor based on the biological effectiveness with short irradiation interruption (f_{add}) is obtained as follows:

$$f_{add} = \frac{D_{1,phy}^{w/o}}{D_1} \quad (21)$$

Results

Validation of the MKM in survival fractions with different oxygen distributions

Figure 1 shows the validation of the survival curves by comparison with the experimental data. The calculation was in good agreement with the measured data for oxygen levels of 0%, 0.5%, and 20%.

Biological dose difference for the short irradiation interruption

Figures 2ADGJMP show the comparison of Δ between IDF of 10–90% for the D of 2 Gy at oxygen levels of 0.075, 3, 8, 15, 38, and 160 mm Hg, respectively. The maximum occurred for the IDF of 50%.

The Δ exceeding 3%, which is typically used in dose distribution measurements, between IDF of 50% and either 10% or 90% occurred more than $\tau = 50$ min in the range of 0.075–160 mm Hg, $\tau = 20$ min in the range of 3–160 mm Hg, $\tau = 20$ min at 8 mm Hg, $\tau = 20$ min in the range of 15–160 mm Hg, $\tau = 20$ min in

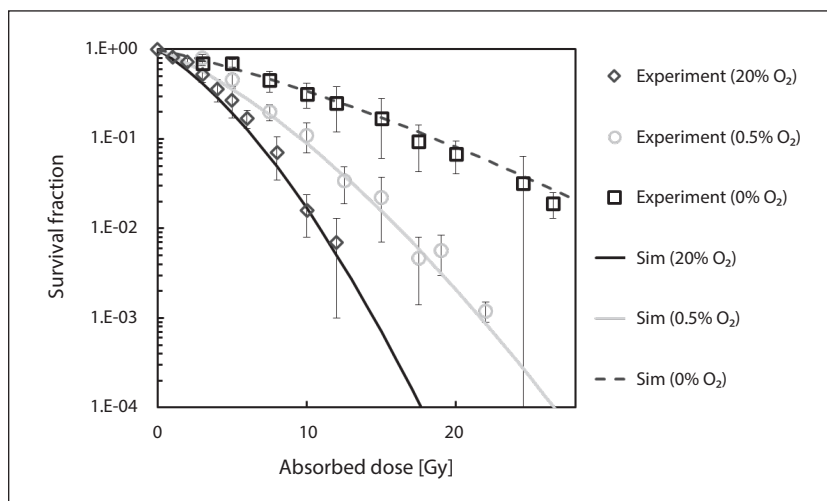


Figure 1. Survival fractions in calculation with particle and heavy ion transport code system (PHITS) and the experiment data

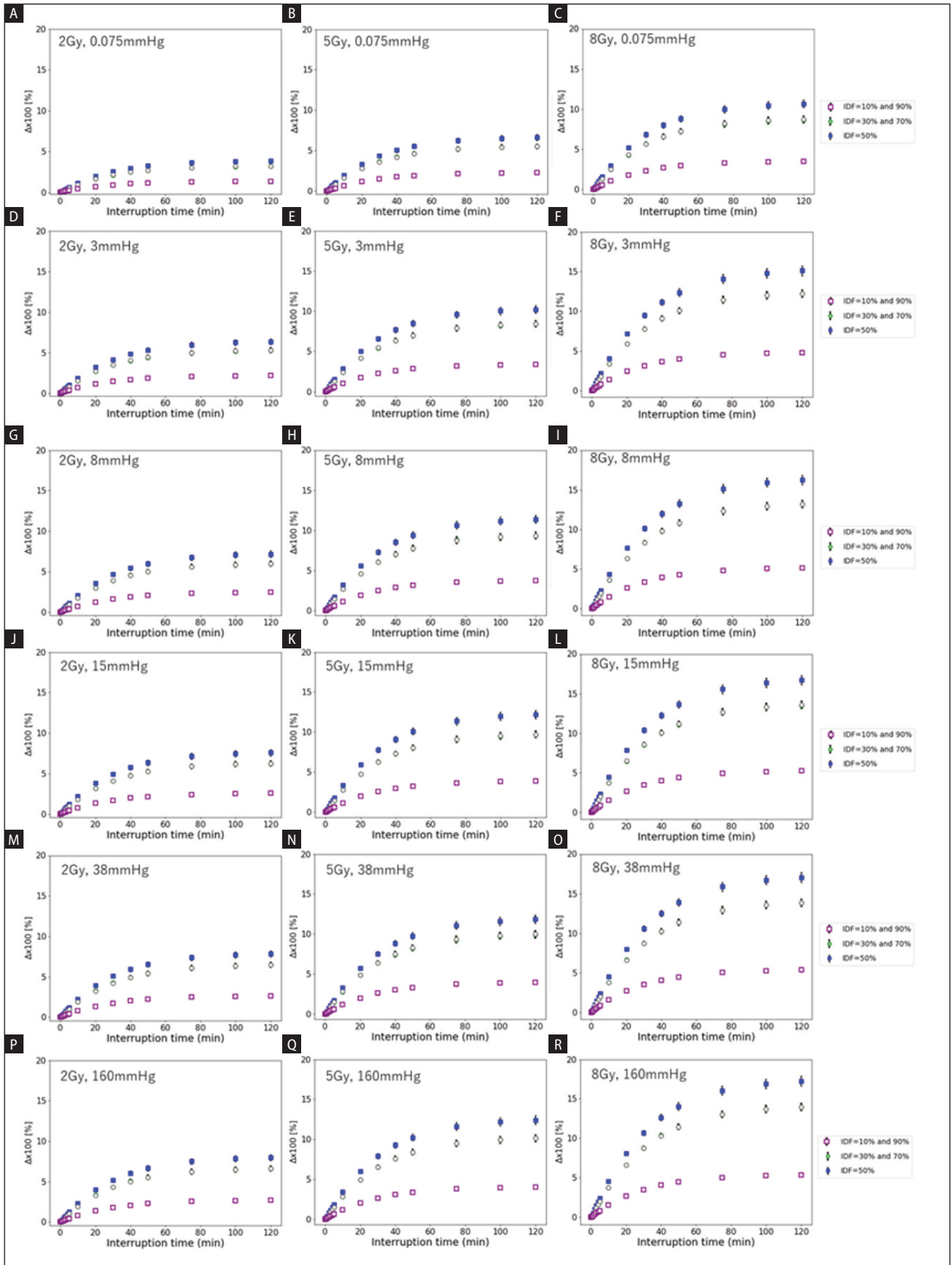


Figure 2. when short irradiation interruption occurs with the IDF of 10–90% for the D of 2 Gy, 5 Gy, and 8 Gy at oxygen levels of 0.075 (A–C), 3 (D–F), 8 (G–I), 15 (J–L), 38 (M–O), and 160 (P–R) mm Hg

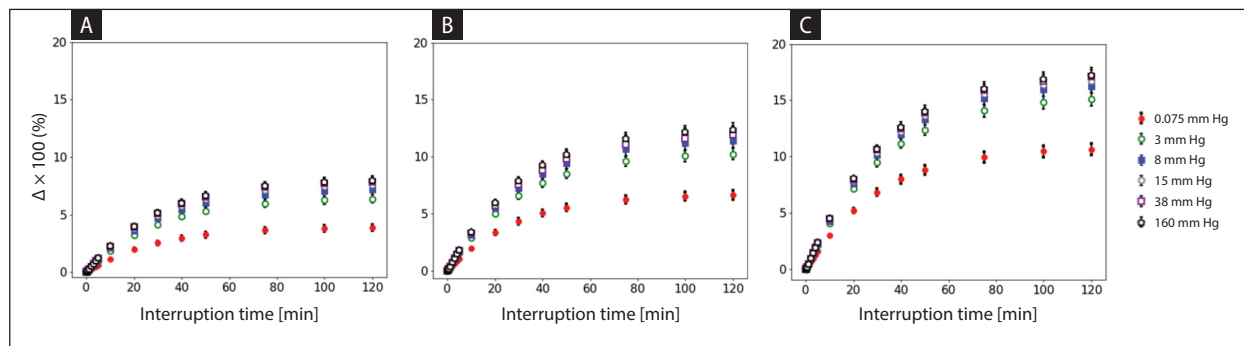


Figure 3. when the short irradiation interruption occurs at oxygen levels of 0.075, 3, 8, 15, 38, and 160 mm Hg with IDF of 50% for the D of (A) 2 Gy, (B) 5 Gy, and (C) 8 Gy

the range of 38–160 mm Hg, and $\tau = 20$ min at 160 mm Hg [18]. The maximum Δ between IDF of 50% and either 10% or 90% was 3.8% at 0.075 mm Hg, 6.2% at 3 mm Hg, 7.0% at 8 mm Hg, 7.3% at 15 mm Hg, 7.6% at 38 mm Hg, and 7.7% at 160 mm Hg. Figures 2BEHKNQ show the comparison of Δ between IDF of 10–90% for the D of 4 Gy at oxygen levels of 0.075, 3, 8, 15, 38, and 160 mm Hg, respectively. The Δ at more than 3% between IDF of 50% and either 10% or 90% occurred more than $\tau = 20$ min at 0.075 mm Hg, $\tau = 10$ min at 3 mm Hg, $\tau = 10$ min at 8 mm Hg, $\tau = 10$ min at 15 mm Hg, $\tau = 10$ min at 38 mm Hg, and $\tau = 10$ min at 160 mm Hg. The maximum Δ between IDF of 50% and either 10% or 90% was 6.6% at 0.075 mm Hg, 10.2% at 3 mm Hg, 11.4% at 8 mm Hg, 11.9% at 15 mm Hg, 12.2% at 38 mm Hg, and 12.4% at 160 mm Hg for the D of 4 Gy. Figures 2CFILOR show the comparison of Δ between IDF of 10–90% for the D of 8 Gy at oxygen levels of 0.075, 3, 8, 15, 38, and 160 mm Hg, respectively. The Δ at more than 3% between IDF of 50% and either 10% or 90% occurred more than $\tau = 10$ min at 0.075 mm Hg, $\tau = 10$ min at 3 mm Hg, $\tau = 10$ min at 8 mm Hg, $\tau = 10$ min at 15 mm Hg, $\tau = 10$ min at 38 mm Hg, and $\tau = 10$ min at 160 mm Hg. The maximum Δ between IDF of 50% and either 10% or 90% was 10.7% at 0.075 mm Hg, 15.1% at 3 mm Hg, 16.3% at 8 mm Hg, 16.7% at 15 mm Hg, 17.1% at 38 mm Hg, and 17.3% at 160 mm Hg. The Δ value was smaller for lower IDF and lower dose. The maximum Δ occurred at the oxygen level of 160 mm Hg with 8 Gy.

Figure 3 shows the comparison of Δ at the oxygen levels of 0.075, 3, 8, 15, 38, and 160 mm Hg with IDF of 50% for the D of 2–8 Gy. The Δ value was

the smallest at 0.075 mm Hg. The Δ at more than 3% between 0.075 mm Hg and 3–160 mm Hg occurred more than 4 min for the D of 2 Gy, 3 min for the D of 4 Gy, and 3 min for D of 8 Gy. The Δ value was higher for high oxygen levels. The Δ at oxygen levels of 3–160 mm Hg was within 2.2% for 2–8 Gy.

Dose compensating factor with different fraction of the interrupted dose

Figure 4 shows at 1 Gy/min for the D of 2–8 Gy at oxygen levels of 0.075, 3, 8, 15, 38, and 160 mm Hg. The was larger with the and dose per fraction. Although the was larger with a higher rate of IDF, the difference in the with IDF = 10% and 30% was within 3%. Similar to the relation of the oxygen concentration and the , the high concentration of oxygen had a higher. The at an oxygen level > 8 mm Hg was within 1.0% at each IDF and interruption time.

Discussion

In a previous study, we evaluated the unexpected decrease in biological effectiveness with short irradiation interruptions using MKM [17]. This study improved the MKM to estimate the biological dose for each oxygen condition. The biological dose difference, with and without short irradiation interruptions, increased with increasing oxygen concentration. However, the Δ at oxygen levels of 3–160 mm Hg for each interruption time was within 2.2% for 2–8 Gy. Shibamoto et al. reported that the effect of radiation decreased by 9–14% at 8 Gy for radiosurgery when the total radiation time was between 20 and 30 min with some intervals [17]. Although we assumed irradiation in-

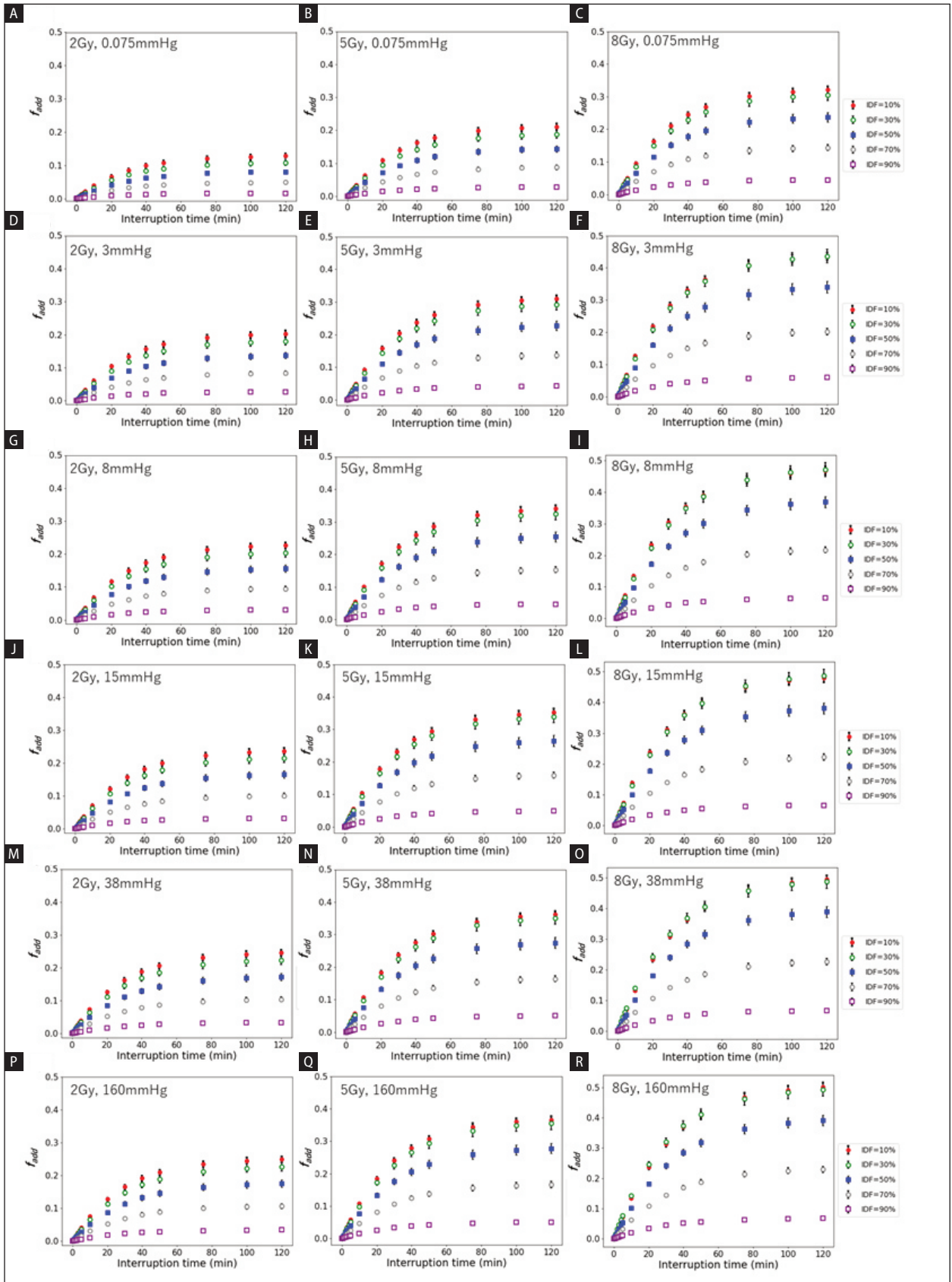


Figure 4. when the short irradiation interruption occurs with the IDF of 10–90% for the D of (A) 2 Gy, (B) 5 Gy, and (C) 8 Gy at oxygen levels of 0.075 (A–C), 3 (D–F), 8 (G–I), 15 (J–L), 38 (M–O), and 160 (P–R) mm Hg

interruption, our findings showed a comparable decrease in the Δ for oxygen levels of 3–160 mm Hg. Conversely, the Δ with and without a short irradiation interruption of more than 3% between 0.075 mm Hg and 3–160 mm Hg occurred for more than 4 min for 2 Gy, 3 min for 4 Gy, and 3 min for 8 Gy. Tumor hypoxia promotes malignancy and resistance to treatment, implying that hypoxia diminishes the biological effectiveness relative to the physical dose.

McKeown et al. reported that hypoxia caused tumor cell death only when the oxygen level was 0.075 mm Hg for more than 24 h [14]. Tumors induce apoptosis, resulting in decreased chromatin condensation, colony formation, caspase activation, and DNA fragmentation. This study did not consider apoptosis in the simulations.

The median oxygen level is > 1.0% for brain, head and neck, lung, and breast cancers [14]. The at an oxygen level > 8 mm Hg (1.0%) was within 1.0%; this can unify the biological compensation factor model. In contrast, the median oxygen level has been reported to be within an oxygen level of 8 mm Hg in liver, pancreatic, and prostate cancers. Dose compensation should be performed after evaluating the microregional oxygen levels.

Recently, FLASH therapy was shown to reduce irradiation time and increase radioresistance in hypoxic cells. Adrian et al. reported that cells began to exhibit hypoxic behavior after FLASH irradiation, indicating that the biological effectiveness with and without short irradiation interruptions might be reduced [19].

In this study, short irradiation interruptions were assumed to occur during the first irradiation. The dose profiles for the first and subsequent irradiations were identical. In a clinical setting, the dose compensation factor should be applied to the remaining physical dose from the first irradiation for each voxel.

Conclusions

Short irradiation interruption caused a loss of biological effects. The dose compensation model corrected an unexpected decrease in biological effectiveness with a short irradiation interruption time.

Conflict of interest

Author declare no conflict of interest.

Acknowledgements

None.

Funding

None declared.

References

- Staffurth J. Radiotherapy Development Board. A review of the clinical evidence for intensity-modulated radiotherapy. *Clin Oncol (R Coll Radiol)*. 2010; 22(8): 643–657, doi: [10.1016/j.clon.2010.06.013](https://doi.org/10.1016/j.clon.2010.06.013), indexed in Pubmed: [20673708](https://pubmed.ncbi.nlm.nih.gov/20673708/).
- Veldeman L, Madani I, Hulstaert F, et al. Evidence behind use of intensity-modulated radiotherapy: a systematic review of comparative clinical studies. *Lancet Oncol*. 2008; 9(4): 367–375, doi: [10.1016/S1470-2045\(08\)70098-6](https://doi.org/10.1016/S1470-2045(08)70098-6), indexed in Pubmed: [18374290](https://pubmed.ncbi.nlm.nih.gov/18374290/).
- Otto K. Volumetric modulated arc therapy: IMRT in a single gantry arc. *Med Phys*. 2008; 35(1): 310–317, doi: [10.1118/1.2818738](https://doi.org/10.1118/1.2818738), indexed in Pubmed: [18293586](https://pubmed.ncbi.nlm.nih.gov/18293586/).
- Verbakel WF, van den Berg J, Slotman BJ, et al. Comparable cell survival between high dose rate flattening filter free and conventional dose rate irradiation. *Acta Oncol*. 2013; 52(3): 652–657, doi: [10.3109/0284186X.2012.737021](https://doi.org/10.3109/0284186X.2012.737021), indexed in Pubmed: [23126524](https://pubmed.ncbi.nlm.nih.gov/23126524/).
- Lohse I, Lang S, Hrbacek J, et al. Effect of high dose per pulse flattening filter-free beams on cancer cell survival. *Radiother Oncol*. 2011; 101(1): 226–232, doi: [10.1016/j.radonc.2011.05.072](https://doi.org/10.1016/j.radonc.2011.05.072), indexed in Pubmed: [21733592](https://pubmed.ncbi.nlm.nih.gov/21733592/).
- Nakano H, Kawahara D, Ono K, et al. Effect of dose-delivery time for flattened and flattening filter-free photon beams based on microdosimetric kinetic model. *PLoS One*. 2018; 13(11): e0206673, doi: [10.1371/journal.pone.0206673](https://doi.org/10.1371/journal.pone.0206673), indexed in Pubmed: [30462672](https://pubmed.ncbi.nlm.nih.gov/30462672/).
- Kawahara D, Nakano H, Saito A, et al. Dose compensation based on biological effectiveness due to interruption time for photon radiation therapy. *Br J Radiol*. 2020; 93(1111): 20200125, doi: [10.1259/bjr.20200125](https://doi.org/10.1259/bjr.20200125), indexed in Pubmed: [32356450](https://pubmed.ncbi.nlm.nih.gov/32356450/).
- Hall EJ, Giaccia AJ. *Radiobiology for the radiologist*. 7th ed. Lippincott Williams & Wilkins 2012: 1–576.
- Tinganelli W, Ma NY, Von Neubeck C, et al. Influence of chronic hypoxia and radiation quality on cell survival. *J Radiat Res*. 2013; 54 Suppl 1(Suppl 1): i13–i22, doi: [10.1093/jrr/rrs135](https://doi.org/10.1093/jrr/rrs135), indexed in Pubmed: [23824117](https://pubmed.ncbi.nlm.nih.gov/23824117/).
- Inaniwa T, Kanematsu N, Suzuki M, et al. Effects of beam interruption time on tumor control probability in single-fractionated carbon-ion radiotherapy for non-small cell lung cancer. *Phys Med Biol*. 2015; 60(10): 4105–4121, doi: [10.1088/0031-9155/60/10/4105](https://doi.org/10.1088/0031-9155/60/10/4105), indexed in Pubmed: [25933161](https://pubmed.ncbi.nlm.nih.gov/25933161/).
- Hawkins RB. A microdosimetric-kinetic model of cell death from exposure to ionizing radiation of any LET, with experimental and clinical applications. *Int J Radiat Biol*. 1996; 69(6): 739–755, doi: [10.1080/095530096145481](https://doi.org/10.1080/095530096145481), indexed in Pubmed: [8691026](https://pubmed.ncbi.nlm.nih.gov/8691026/).
- Matsuya Y, McMahan SJ, Ghita M, et al. Intensity Modulated Radiation Fields Induce Protective Effects and Reduce Importance of Dose-Rate Effects. *Sci Rep*. 2019; 9(1): 9483, doi: [10.1038/s41598-019-45960-z](https://doi.org/10.1038/s41598-019-45960-z), indexed in Pubmed: [31263149](https://pubmed.ncbi.nlm.nih.gov/31263149/).

13. Paul-Gilloteaux P, Potiron V, Delpon G, et al. Optimizing radiotherapy protocols using computer automata to model tumour cell death as a function of oxygen diffusion processes. *Sci Rep.* 2017; 7(1): 2280, doi: [10.1038/s41598-017-01757-6](https://doi.org/10.1038/s41598-017-01757-6), indexed in Pubmed: [28536438](https://pubmed.ncbi.nlm.nih.gov/28536438/).
14. McKeown SR. Defining normoxia, physoxia and hypoxia in tumours-implications for treatment response. *Br J Radiol.* 2014; 87(1035): 20130676, doi: [10.1259/bjr.20130676](https://doi.org/10.1259/bjr.20130676), indexed in Pubmed: [24588669](https://pubmed.ncbi.nlm.nih.gov/24588669/).
15. Brenner DJ, Hlatky LR, Hahnfeldt PJ, et al. The linear-quadratic model and most other common radiobiological models result in similar predictions of time-dose relationships. *Radiat Res.* 1998; 150(1): 83–91, indexed in Pubmed: [9650605](https://pubmed.ncbi.nlm.nih.gov/9650605/).
16. Kawahara D, Nakano H, Ozawa S, et al. Relative biological effectiveness study of Lipiodol based on microdosimetric-kinetic model. *Phys Med.* 2018; 46: 89–95, doi: [10.1016/j.ejmp.2018.01.018](https://doi.org/10.1016/j.ejmp.2018.01.018), indexed in Pubmed: [29519415](https://pubmed.ncbi.nlm.nih.gov/29519415/).
17. Shibamoto Y, Ito M, Sugie C, et al. Recovery from sublethal damage during intermittent exposures in cultured tumor cells: implications for dose modification in radiosurgery and IMRT. *Int J Radiat Oncol Biol Phys.* 2004; 59(5): 1484–1490, doi: [10.1016/j.ijrobp.2004.04.039](https://doi.org/10.1016/j.ijrobp.2004.04.039), indexed in Pubmed: [15275736](https://pubmed.ncbi.nlm.nih.gov/15275736/).
18. Hussein M, Clark CH, Nisbet A. Challenges in calculation of the gamma index in radiotherapy — Towards good practice. *Phys Med.* 2017; 36: 1–11, doi: [10.1016/j.ejmp.2017.03.001](https://doi.org/10.1016/j.ejmp.2017.03.001), indexed in Pubmed: [28410677](https://pubmed.ncbi.nlm.nih.gov/28410677/).
19. Adrian G, Konradsson E, Lempart M, et al. The FLASH effect depends on oxygen concentration. *Br J Radiol.* 2020; 93(1106): 20190702, doi: [10.1259/bjr.20190702](https://doi.org/10.1259/bjr.20190702), indexed in Pubmed: [31825653](https://pubmed.ncbi.nlm.nih.gov/31825653/).